Anal. Bioanal. Electrochem., Vol. 8, No. 3, 2016, 287-303

Analytical & Bioanalytical Electrochemistry

2016 by CEE
www.abechem.com

Full Paper

An Au-Pd@MWCNT/graphene Modified Carbon Paste Electrode as a Novel Nano-Composite Sensor for the Trace Determination of Nitrite

Mosayeb Rezaei*

Young Researchers and Elite Club, Hamedan Branch, Islamic Azad University, Hamedan, Iran

*Corresponding Author, Tel.: +98 813 826 3283; Fax: +98 813 826 3283

E-Mail: Mosayebrezaei@gmail.com

Receive: 8 March 2016 / Accepted: 20 April 2016 / Published online: 15 May 2016

Abstract- This paper has presented a novel strategy to carry out the direct and sensitive determination of nitrite ion in different and complex matrices based on a new nano-composite carbon paste electrode composed of (Au-Pd@MWCNT/Gr)-CPE. The characteristics of the proposed nano-materials were investigated by scanning electron microscopy and X-ray diffraction. The effects of various experimental parameters on the electrochemical response of the nitrite ions were assayed and optimized. Under the optimized conditions, the calibration curve for nitrite ion concentration was linear in the range of 0.02-55.0 µmol L^{-1} with the detection limit of 9.44 nmol L^{-1}. In addition, the suggested sensor was successfully applied to the determination of nitrite ion in sausages, cheese, plant foodstuffs, soil, mineral water and tap water samples with satisfactory results. However, the prepared sensor may hold great promise for fast, simple and sensitive detection of nitrite in various real samples.

Keywords- Nitrite, CPE, Au-Pd bimetallic, MWCNT, Graphene

1. INTRODUCTION

As we know, Nitrogen species such nitrites play an important role in determining the ecological status and health of freshwater ecosystems. They are one of the most implicated species in water eutrophication. Nowadays, nitrite was dramatically used in food, corrosion

industrial and agriculture and has an active role in the oxidation of ammonia or reduction of nitrates [1,2]. Nitrite is present in foodstuff as a preservative (such in different kinds of meat and cheese) or as a natural component (such in vegetables). It is also found in water due to chloramination, which may give rise to the formation of nitrite within the water distribution system. The concentration of nitrite may increase as the water moves towards the extremities of the network. The maximum value of nitrite in potable water is 2.17 μmol L^{-1} [3].

However, The World Health Organization (WHO) has reported that the fatal dose of nitrite ingestion is between 8.7 μM and 28.3 μM depending on body weight and it has been classified as a human health- hazard [3,4].

It has been reported when the level of nitrite increase into the blood, an irreversible oxidation of hemoglobin to methemoglobin will occur and the Fe^{2+} present in the haem group is oxidized to its Fe^{3+} form, the Fe^{3+} form does not allow oxygen transport, in result oxygen carrying capacity of blood have fallen sharply which leads to a condition commonly called “blue baby syndrome [5]. Moreover, nitrite can react with amines and amides, then N-nitrosoamines was formed as a carcinogen [6].

It is, therefore, due to potential toxicity of nitrite, important to develop the simple, selective, sensitive, efficient and eco-friendly methods for the determination trace levels of nitrite in environmental, food and biological samples.

Various instrumental techniques have been employed for the determination of nitrite ion in different real samples, including spectrophotometry [7,8], spectrofluorimetry [9,10], capillary electrophoresis chemiluminescence [11], chromatography [12,13], flow injection Analysis [14]. However, instrumental methods have disadvantages such as the toxicity of used reagents, time-consuming extraction processes and the presence of serious interferences. Electrochemical methods due to faster, cheaper and simpler are often favored over others [15, 16].

Therefore, several kinds of chemically modified electrodes (CMEs) have been designed and utilized by various materials for determination of ions and molecules and especially selective determination of trace amount of nitrite [17-22]. The development and application of CMEs have received considerable attention in recent years. CMEs are characterized by purposefully altering their surface characteristics to display new qualities that can be exploited for analytical purposes. The huge success of CMEs arises most often from the remarkable and sometimes unique properties of the modifiers [23]. Among these electrodes, carbon-paste electrodes (CPEs), due to the ease of their construction, easy renewability of the surface, wider potential window according to experimental conditions and compatibility with various types of modifiers, have been widely used as suitable matrices for the construction of the modified electrodes.

Nowadays, due to the need for the improvements in sensing characteristics of electrodes, such as selectivity, stability, and cost-effectiveness, new sensing layers has been studied to

improve detection in chemical sensing and biosensing. To further improve the sensitivity of the electrochemical sensor, more electrocatalytic sites, and low resistant are required on the modified electrode. Nanomaterials, such as carbon nanotubes (CNTs) [24-27], graphene [28-30], metal nanoparticles [31,32], and metal oxide [33-35], can greatly enhance the analytical performance of sensors. The researchers for novel matrices became the subject of increasing interest. Since the discovery of multiwalled carbon nanotubes (MWCNTs) by Iijima [36]. These materials have attracted enormous interest because of their novel structure, narrow distribution size, highly accessible surface area, low resistance and high stability. Electrochemical sensors based on MWCNTs represent a new and interesting alternative for the quantification of different analytes. It has been concluded that introduction of MWCNTs into a carbon paste improves the electric conductivity as well as the mechanical properties of the original paste matrix. In addition, MWCNTs have a role to enhance the hydrophobicity of the surface, which leads to a more stable potential signal by removing the undesirable water layer from the interface [37].

At the same time, the search for novel matrices became the subject of increasing interest. Graphene due to its unique physicochemical properties such as high specific surface area, chemical stability and electrical conductivity, excellent thermal conductivity, and strong mechanical strength, has attracted strong scientific and technological interest in recent years [38-40]. For the potential application of a certain kind of carbon material in electrochemistry, the basic electrochemical behaviors should be first studied to determine several important parameters of carbon sensors [38] including electrochemical potential window and heterogeneous electron transfer rate. Therefore, possible routes to harnessing these excellent properties of graphene for applications will be to incorporate graphene into a composite material [41] and also the graphene has begun to be exploited as an alternative choice for electrical sensors, especially during the fabrication of electrochemical sensing devices [39].

Also, bimetallic nanoparticles show wide variety favorable properties compared with corresponding monometallic counterparts, which include high catalytic activity, catalytic selectivity, and better resistance to deactivation [42-47]. Given that bimetallic nanoparticles have been shown to increase the electrode areas that could bring in more molecular recognition elements to improve the sensitivity of the sensor. In addition, decorating MWCNTs with nanoparticles leads to enhance in signal response [48,49]. Au-Pd nanoparticle was used in many reactions such as hydrogenation reactions [50], degradation reactions [51], oxidation reactions [52] and hydrogenation of hydrocarbon [53] because their special properties such as high catalytic performance. Modified electrodes with Au-Pd bimetallic nanoparticle have exclusive features such as high sensitivity, fast response time, wide linear range, better selectivity, and reproducibility becomes significant [54-57].

In this study, a simple and rapid electrochemical method based on the square wave voltammetry (SWV) for the direct determination of nitrite at an (Au-Pd@MWCNT/Gr)-CPE

was suggested. The modified electrode, due to unique properties of Au-Pd@MWCNT and Gr such as high surface-to-volume ratio, high catalytic efficiency, good biocompatibility and chemical stability was used for the determination of nitrite in the various real samples.

2. EXPERIMENTAL

2.1. Materials

All chemicals and reagents used in this work were of analytical grade and used as received without further purification. Sodium nitrite as target analyte, Sodium hydrogen phosphate, disodium hydrogen phosphate, $HAuCl_4$, K_2PdCl and sodium hydroxide, paraffin oil and graphite powder were used as the composition of electrodes were purchased from Merck Company. Stock solutions of 1.0×10^{-2} mol L^{-1} nitrite were freshly prepared as required. Deionized distilled water (DDW) was used to prepare all the solutions. Phosphate buffer solutions with different pH values were prepared from a solution that contains 0.10 mol L^{-1} Na_2HPO_4 and 0.10 mol L^{-1} NaH_2PO_4, while pH values were adjusted by addition of 1.0 mol L^{-1} H_3PO_4 and/or NaOH solution.

2.2. Apparatus

Behpajoh potentiostat/galvanostat system (model BHP-2065) was employed for all the voltammetric measurements including cyclic voltammetry (CV) and SWV. A conventional three-electrode system assembly including a platinum wire (auxiliary electrode), an Ag/AgCl as a reference electrode and CPEs (unmodified and modified) as working electrodes were used. The morphological characterizations of all electrodes have been examined by means of scanning electrochemical microscopy, SEM (SEM-EDX, Philips Netherland). X-ray powder diffraction (XRD, 38066 Riva, d/G.Via M. Misone, 11/D (TN) Italy) was employed to analyze the chemical components of the composites. The pH-measurements were done with a Metrohm pH meter (model 713).

2.3. Pretreatment of Multiwalled Carbon Nanotubes

A pretreatment of the MWCNTs is usually necessary to eliminate graphitic nanoparticles, amorphous carbon, metallic impurities, and/or to improve the electron transfer properties and/or to allow further functionalization. The pretreatment consists in exposing the MWCNTs to an acidic solution of sulfuric, nitric or hydrochloric acid, or a mixture of these acids at room temperature, under refluxing or under sonication for different times. Following one of the purification methodologies, 500 mg of MWCNTs was heated at 400 ^oC using an air flow of 12 mL min^{-1} (quartz tubular reactor of 14 mm diameter), for 1 h [48,58,59]. To eliminate metal oxide catalysts, the heated processed amount of MWCNTs were dispersed in

60 mL of 6.0 mol L^{-1} HCl for 4 h under ultrasonic agitation; filtered on a Whattman No. 42 filter paper and washed until the pH of the solution was neutral; and finally, dried.

2.4. Preparation of Au-Pd@MWCNT nano-composite

The Au-Pd nanoparticles were synthesized according to the literature [60]. Typically, 1 mL of a 5 mM aqueous solution of an $HAuCl_4/K_2PdCl$ mixture (molar ratios of 1:1) was added to 47 mL of purified water. Then ascorbic acid (100 mM, 50 mL) was added to the mixed solution. After 15 s, an aqueous solution of polyvinyl pyrrolidone (5 mg mL^{-1}, 1 mL) added dropwise with vigorous stirring. After addition, the mixture was stirred at 25 ^oC for another 1 h and then transferred into 1 mL centrifugal tubes. The obtained Au-Pd nanoparticles were collected by centrifugation at 12,000 rpm for 10 min and washed three times with DDW.

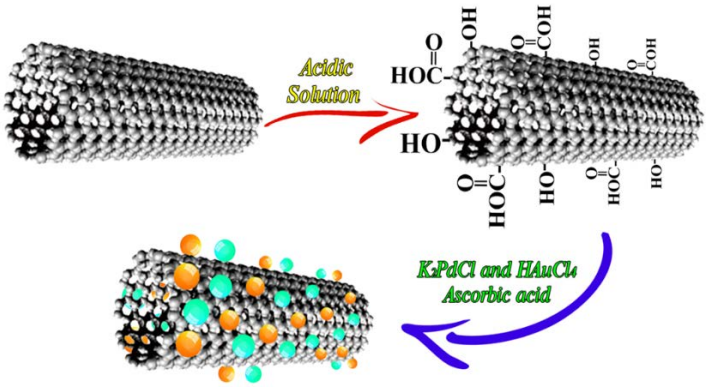

Scheme 1. Synthesis of Au-Pd@MWCNT

For the synthesis of Au-Pd@MWCNT, 2 mL of MWCNT suspension was mixed with an aqueous $HAuCl_4$ and K_2PdCl solution (molar ratios of 1:1) and kept under stirring for 20 min after which ascorbic acid (4 mL, 1 M) was added. Finally, balanced amount of water was added to achieve a final reaction volume of 40 mL. The entire reaction mixture was stirred at 25 °C for 48 h to produce MWCNT decorated with bimetallic Au-Pd nanoparticles (scheme 1).

2.5. Preparation of the modified sensors

Bare CPE was prepared by thorough hand mixing of graphite powder with appropriate amount of paraffin oil at a ratio of 75:25 (w/w) in an agate mortar and grounded homogeneously.

The (MWCNT)-CPE was prepared by mixing 10% (w/w) MWCNTs, 65% (w/w) graphite powder and 25% (w/w) paraffin oil in a mortar and pestle. The Au-Pd/CPE and (Au-

Pd@MWCNT)-CPE were prepared by mixing the unmodified mixture with 10% w/w Au-Pd bimetallic nanoparticles and Au-Pd@MWCNT, respectively. Finally, the (Au-Pd@MWCNT/Gr)-CPE was prepared by mixing 10% w/w Au-Pd@MWCNT, 25% w/w Gr, 40% w/w graphite powder and 25% (w/w) paraffin oil. A copper wire was inserted through the composite end of the working electrode to establish electrical contact.

The each of resulting paste mixtures (prepared by the above-mentioned method) was transferred into an insulin syringe with an internal diameter of 2.5 mm and a height of 3 cm as an electrode body. After the homogenization of each mixture, a portion of the prepared paste was carefully packed into the tube tip to avoid possible air gaps, which often enhance the electrode resistance. A copper wire was inserted into the opposite end of the each CPE to establish electrical contact. Prior to use, the external surface of the carbon paste was smoothed with a soft paper. A new surface was produced by scraping out the old surface and replacing the new carbon paste.

2.6. Preparation of real samples

The extraction of nitrite from sausages and cheese samples (weight of sample taken was 65.8 g and 30 g, respectively) was accomplished by leaving a certain amount of crushed sample in deionized water at 70 ^{o}C under stirring for 10 min and further filtering of the remaining liquid [48].

Plant foodstuffs were purchased from local markets in Hamedan. About 1.000 g of the plant foodstuff was first ashed for 6 h at 500 ^{o}C in a crucible. After cooling, the ash was carefully moistened with 5 mL of 1:1 concentrated nitric acid:H_2O and the mixture were heated on a hotplate to near dryness. The residue was dissolved in 20 mL of DDW. The solution was filtered using filter paper (Whatman No. 1) and the filtration was collected into a 50.0 mL volumetric flask and diluted to the mark with DDW [61].

Soil samples were collected from different sites of an agricultural land. The soil samples were mixed carefully, then an amount equivalent to 30 g of the soil sample was dried at 60 ^{o}C for 2 h in an oven. The dried soil was dissolved in 200 mL of deionized water. The produced solution was then filtered through a Whatman No. 41 filter paper and centrifuged for 30 min, and again filtered through the filter paper, the filtered solution was collected into a 250 mL volumetric flask and diluted to the mark with DDW [62]. The water samples (mineral and tap water) were directly used with any preparation.

3. RESULTS AND DISCUSSION

3.1. Surface characterization

Morphologies of the typical products were investigated by SEM and XRD. The particle size of Au-Pd bimetallic nanoparticles and Au-Pd@MWCNT were investigated from SEM

micrographs. Fig. 1 shows the SEM and XRD of the MWCNT, Au-Pd bimetallic nanoparticles, and Au-Pd@MWCNT. The SEM image of MWCNT displayed a typical morphology of the MWCNT (Fig. 1a). Fig. 1b displays the SEM image of the Au-Pd bimetallic, it can be seen that the size of spherical Au-Pd nanoparticles was about 50–75 nm. Fig. 1c shows Au-Pd@MWCNT, while Au-Pd bimetallic were located at uniform size over the MWCNT.

The typical XRD profile of MWCNT, Au-Pd bimetallic nanoparticles and Au-Pd@MWCNT are shown in Fig. 1d. It can be seen that the MWCNTs displayed a typical characteristic (002) peak at a 2θ value of about 26° that is referred to graphite plate of MWCNTs.

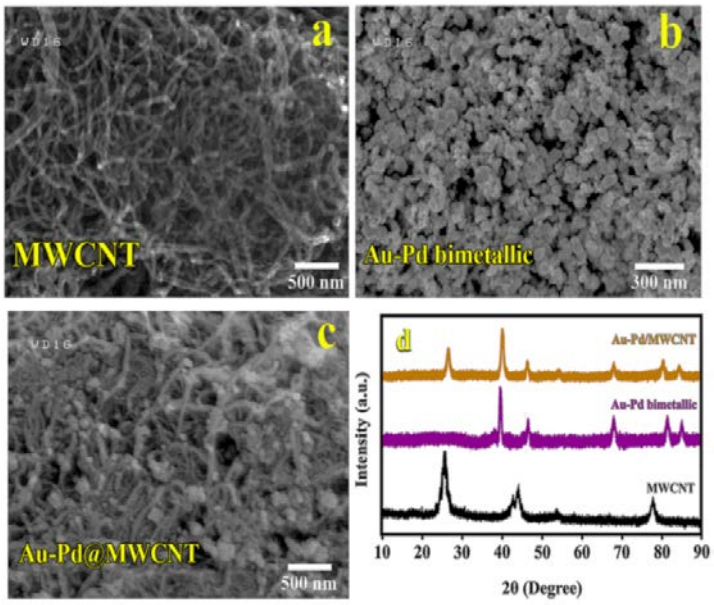

Fig. 1. SEM images from surface of (a) MWCNT; (b) Au-Pd bimetallic; (c) Au-Pd@MWCNT and (d) XRD patterns of MWCNT, Au-Pd bimetallic and Au-Pd@MWCNT

In the XRD pattern of the Au-Pd nanoparticles, the peaks at 38.9◦, 45.6◦, 67.1◦, 81.9 and 85.3◦, corresponding to the (1 1 1), (2 0 0), (2 2 0), (3 1 1) and (2 2 2), respectively, facets of Au-Pd crystal, that are shifted from those of pure Au and Pd crystals (good agreement with the standard JCPDS Card No. 05-0681 for Pd and the standard JCPDS Card No. 04-0784 for Au). These peaks indicate the coexistence of Au and Pd in the catalyst.

For Au-Pd@MWCNT, the positions of diffraction peaks matched well with standard Au-Pd bimetallic nanoparticles and MWCNT, suggesting that prepared composite composed of pure crystalline Au-Pd bimetallic nanoparticles were successfully decorated onto the MWCNT.

3.2. Electrochemical behaviors of nitrite at different electrodes

The square wave voltammograms (SWVs) were obtained for the unmodified or bare CPE and modified CPEs including (MWCNT)-CPE, Au-Pd/CPE, (Au-Pd@MWCNT)-CPE and (Au-Pd@MWCNT/Gr)-CPE in the presence of nitrite ion solutions (10 µmol L^{-1}) in the buffer solutions (pH=5.0) using a deposition potential of −0.7 V *vs.* Ag/AgCl for 100 s. The results are summarized in Fig. 2.

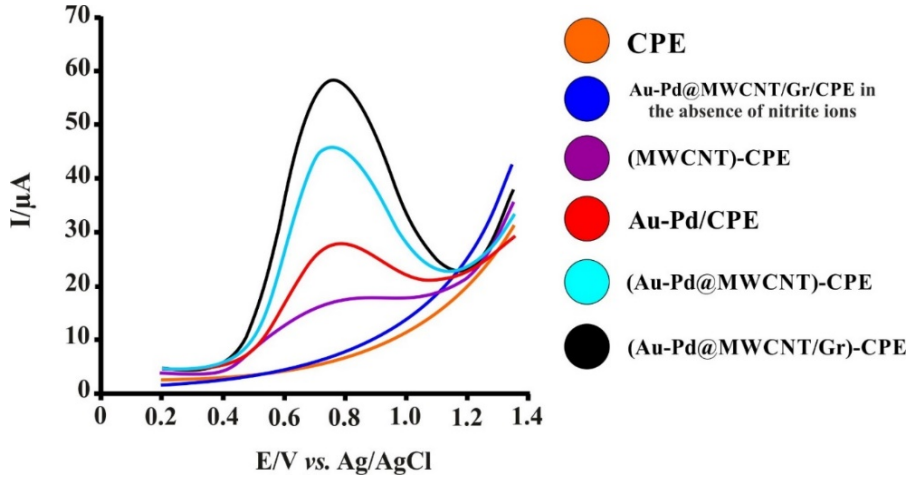

Fig. 2. SWVs of 10 µmol L^{-1} of nitrite on the surface of various sensors. Conditions: pH 5.0; deposition potential, −0.700 V *vs.* Ag/AgCl; deposition time, 100 s; resting time, 10 s

According to Fig. 2, there is no observable peak for an unmodified CPE. However, a broad anodic peak with weak peak current for nitrite is observed on the (MWCNT)-CPE. Moreover, sharp anodic peaks at 0.759 V *vs.* Ag/AgCl on the surface of the Au-Pd/CPE and (Au-Pd@MWCNT)-CPE were observed probably due to the oxidation of nitrite. As can be seen from Fig. 2, the (Au-Pd@MWCNT)-CPE showed a larger anodic peak current than the Au-Pd/CPE because of a decrease in the overpotential of the process at the surface of the (Au-Pd@MWCNT)-CPE, revealed that the (Au-Pd@MWCNT)-CPE could act as an effective promoter to enhance the kinetics of the electrochemical process. By further modification of the (Au-Pd@MWCNT)-CPE with Gr, the anodic peak current of the analyte have a remarkably increased due to the increasing of the surface area of the electrode compared to (Au-Pd@MWCNT)-CPE. However, in the absence of nitrite ion, there is no observable peak at (Au-Pd@MWCNT/Gr)-CPE that indicated the stability of the electrode in the proposed potential scan range.

3.3. Influence of pH and supporting electrolyte on peak current

The effect of the nature of three kinds of supporting electrolytes (Briton–Robinson (B-R), phosphate, and acetate buffer solutions) at different pH values on the voltammetric behavior

of the proposed modified CPE were investigated. Both the peak height and the peak shape were taken into consideration when choosing the supporting electrolyte. Of these, B–R buffer solution gave the best response.

The influence of the solution pH on the peak current was studied using B–R buffers of different pHs between 2.0 and 9.0 and shown in Fig. 3. As can be seen, the peak current increased dramatically by increasing pH up to 5.0, then it has decreased at higher pHs and we can see maximum peak current at pH=5.0. On the other hand, the peak potential for nitrite is not affiliated by pH. It can be attributed to a kinetically controlled oxidation process, i.e. a proton independent catalytic step [63].

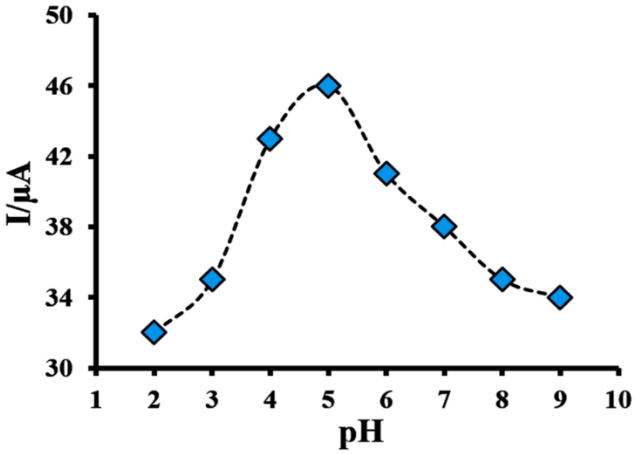

Fig. 3. Influence of buffer pH on peak currents of 5 µmol L^{-1} nitrite

The decreases in current peak at pH values lower than 5.0 can be attributed to the protonation of nitrite ions, or the conversion of NO_2^- to NO in acidic media. Since the pKa of HNO_2 is 3.30, most nitrite anions were protonated in acidic solution. However, the oxidation of nitrite is a proton independent catalytic step. It means that the decrease in nitrite signal at higher pHs has a kinetic reason [47]. Consequently, a compromise value of pH 5.0 was employed for subsequent studies.

3.4. Effect of scan rate on the electrochemical oxidation of nitrite

To investigate the reaction kinetics, the effect of scan rate on the peak currents and peak potentials of nitrite were studied (Fig. 4). Fig. 4b showed that the peak currents changed in a linear relationship with the square root of scan rates in the ranges of 10-400 mV s^{-1} for 10 µmol L^{-1} of nitrite (at pH=5), with R^2 values of above 0.99. These plots indicated that the electrochemical reactions for these molecules were a diffusion-controlled process. In addition, for more investigations, logarithm peak currents versus logarithm scan rates were plotted for the analyte. For these plots when the slope was 0.5, the electrochemical reaction

was a diffusion-controlled process, and when equals to one, the electrochemical reaction occurs via an adsorption-controlled process [64].

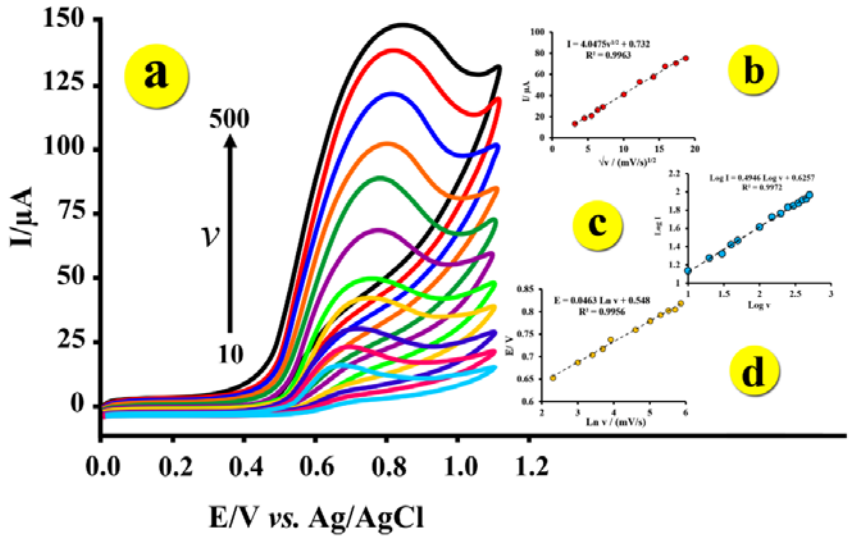

Fig. 4. CVs for (Au-Pd@MWCNT/Gr)-CPE (in B-R buffer solution with pH 5.0) containing 1.5 μmol L^{-1} of nitrite with scan rates ranging from 10 to 500 mV s^{-1} (a). Insets show the linear relationship between the peak current and square root of the scan rate (b) and potential of peaks *vs*. Ln scan rate (c)

The plots of logarithm anodic peak currents versus logarithm scan rates had slopes of 0.4946 for nitrite (Fig. 4c) and this value indicated that the electrochemical reactions for nitrite was governed by diffusion control and they did not foul the surface of (Au-Pd@MWCNT/Gr)-CPE.

It should be noted that the oxidation peak potential (E_{pa}) of nitrite shifted positively with the increase in scan rate (Fig. 4d). Linear relationship between Epa and ln of scan rate was obtained Epa=9.341log *v*-5.1096 (R^2=0.9956), indicating a kinetic limitation in the reaction between the redox sites of APM/GCPE and nitrite.

3.5. Effect of deposition potential, accumulation time and instrumental parameters

It was significant to the investigation of the preconcentration potential and time adsorption. Both parameters could affect the amount of adsorption of nitrite ion at the electrode. So, the effect of deposition potential and accumulation time on SWVs signal were studied with 5 μmol L^{-1} of nitrite ion with the deposition potential from -0.1 to -1.3 V *vs*. Ag/AgCl. It has been noticed that the peak current for nitrite ion exhibits a remarkable dependence on the deposition potential and the largest peak current was obtained at an accumulation potential of −0.7 V *vs*. Ag/AgCl. It can be seen, when deposition potential

become more negative than −0.7 V, the peak currents decreases due to the reduction of other chemicals at these potentials and interfere in the determination of nitrite ion. Furthermore, as the deposition potential becoming more negative, the reproducibility of stripping currents for nitrite ion became poor, because hydrogen evolution was beginning to be significant in the medium at such negative potentials. Also, the nitrite ion deposited on the electrode surface might be damaged by the hydrogen bubble and lead to a decrease in current signals at very negative potentials [19-21].

The effect of deposition time on the stripping responses of nitrite ions was studied under the other optimum conditions from 10 to 120 s and it has been found that the peak currents increase with the increase of preconcentration time from 10 to 100 s. This is due to the fact that longer the preconcentration time caused more and more analyte get accumulated at the electrode/solution interface onto functionalized surface, hence current increases. After 100 s, the peak currents become almost constant due to either surface saturation. Therefore, a preconcentration time of 100 s has been used in all further studies.

In order to obtain well-defined SWV response signals, the voltammetric measurement parameters (pulse amplitude, frequency, resting time and Voltage step) have also been optimized. These parameters were optimized for obtaining maximum signal-to-noise ratio. Optimum values for the studied parameters are given in Table 1.

Table 1. Optimum value for instrumental parameters

Parameter	Range studied	Optimum value
Pulse amplitude (mV)	5-200	100
Frequency (Hz)	5-120	60
Voltage step (mV)	1-10	5
resting time (s)	0-60	10

3.6. Analytical performance, repeatability, reproducibility, and stability

Under the optimal conditions, calibration plot for the determination of nitrite ion at APM/GCPE was obtained by SWV (Fig. 5). As shown in Fig. 5, the peak current was proportional to the concentration of nitrite in the range 0.02 to 55.0 μmol L^{-1}. Also, it can be seen that the oxidation peaks current of nitrite ion increased linearly with the increasing concentrations. The linear regression equation was obtained of I_{pa}=4.5345C (NO_2^-)+1.0253 (R^2=0.9983). Based on the 3Sb/m, which Sb is the standard deviation of blank determinations

and m is the slope of calibration plot, the detection limit for the determination of nitrite ion was found to be 9.4 nmol L^{-1}.

The repeatability, reproducibility, and stability of (Au-Pd@MWCNT/Gr)-CPE were investigated in the B-R buffer solution containing 1.5 µmol L^{-1} of nitrite ion. According to successive measurements in 10 times, the proposed sensor showed an acceptable repeatability with a relative standard deviation of 2.63%, for the oxidation peak currents of the analyte. With ten prepared sensors independently using the same procedure, RSD of 3.34% for oxidation nitrite ion was obtained. Thus, the proposed method had an excellent reproducibility for the determination of nitrite. The modified electrode was stored in ambient at the lab for 28-days. After 7, 14, 21 and 28-days, the anodic peak currents of the sensor, retained more than 99.6%, 98.7%, 97.1% and 93.4% compared with initial value which shows a good stability of electrode for the analysis of real samples.

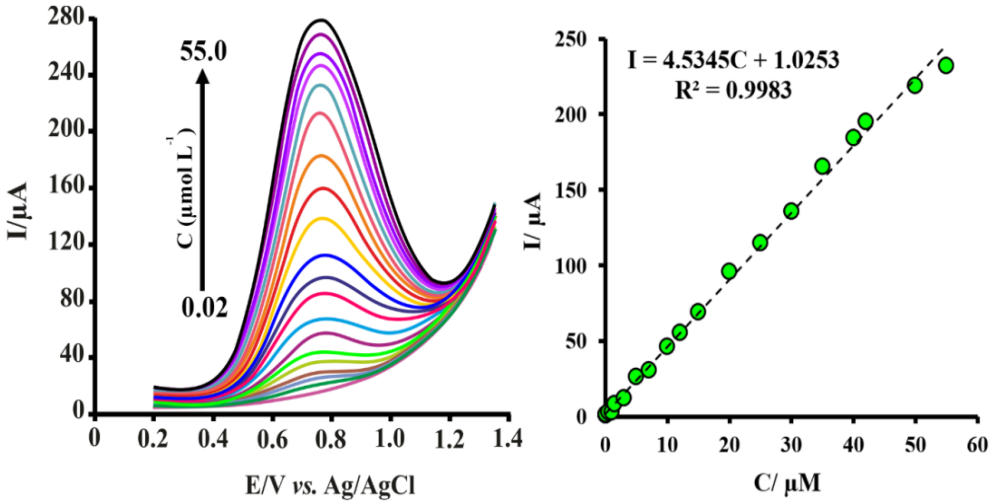

Fig. 5. SWVs for different concentrations of nitrite (0.02–55.0 µmol L^{-1}) in optimum condition

3.7. Selectivity and Interferences study

The interferences of the other species that commonly found with the target analyte in real samples were studied. The response and selectivity of the modified electrode for the determination of nitrite was studied under the optimum conditions with 10.0 µmol L^{-1} of the analyte at pH=5.0. Tolerance limit was taken as the maximum concentration of foreign species that caused an approximate relative error of ±5%. The results are given in Table 2, demonstrated that the modified electrode has a good selectivity for nitrite ion analysis.

The comparison of (Au-Pd@MWCNT/Gr)-CPE with other modified electrodes for the determination of nitrite was listed in Table 3, it could be seen that (Au-Pd@MWCNT/Gr)-CPE had the comparable sensitivities and detection limits for the detection of nitrite ion.

Table 2. Level of interferences on the peak current of nitrite

Interfering species	**Ratio between interference and analyte Interference:Nitrite**
K^+, Na^+ , Mg^{2+}, Ca^{2+}, Zn^{2+}, Cl^-, SO_4^{2-}, SO_3^{2-}, F^-	250:1
NO_3^-, IO_3^-	150:1
Glucose, HOAc, H_2O_2, Ascorbic acid, Uric acid	100:1

Table 3. Comparison of the response characteristics of different modified electrodes.

Electrode	**Method**	**Linear range (µmol L^{-1})**	**Opt. pH**	**Detection limit (µmol L^{-1})**	**Ref.**
Ag–PAMAM/GCE	Amperometry	4-1440	6	0.4	[2]
CoNi NPs/ERGO/GCE[a]	Amperometry	0.10–30 and 30–330	7.98	0.05	[3]
GNPs/MWCPE[b]	SWV	0.05–250.0	4	0.01	[4]
CPE/Cu–PFHA-EDA[c]	CV	0-1380	4.4	5.56	[5]
Ag-GO/GC	LSV	10-180	7.2	2.1	[6]
Au/Cu-MOF/CPE[d]	Amperometry	0.05 -717.2	7.2	0.3	[7]
CoHCF-rGO /GCE	DPV	1-100	6.5	0.27	[8]
CoL/MNSs/CPE	SWV	0.2-30	4.5	0.015	[9]
(Au-Pd@MWCNT/Gr)-CPE	**SWV**	**0.02-55.0**	**5.0**	**0.0094**	**This work**

a- Reduced graphene oxide nanosheets with CoNi bimetallic alloy nanoparticles
b- Multi-wall carbon nanotubes modified carbon paste electrode with gold nanoparticles
c- Modifying a carbon paste electrode (CPE) with copper (II) complexes formed with commercial (PFHA) and ethylenediamine (EDA)
d- Cu-based Metal-organic Framework

3.8. Analytical application

The proposed method was successfully applied to the determination of nitrite ion in real samples with different matrixes. The results are given in table 4. According to this table, the obtained results are comparable with those obtained by Griess method [65]. Thus, the proposed sensor provides a good alternative for the determination of nitrite in different real samples.

Table 4. Results for nitrite determination in various real samples obtained by the proposed method under the optimum conditions

Samples	Added ($\mu g g^{-1}$)	Proposed Method ($\mu g g^{-1}$)	Griess method ($\mu g g^{-1}$)	Recovery (%)
Sausages	0.00	18.25±0.87	18.32±0.84	-
	10.00	28.36±0.99	28.40±0.85	101.1
Cheese	0.00	0.76±0.08	0.73±0.09	-
	2.00	2.80±0.10	2.77±0.11	102
Plant foodstuffs	0.00	14.19±0.66	14.23±0.57	-
	10.00	24.23±1.10	24.31±1.12	100.4
Soil	0.00	0.51±0.09	0.49±0.10	-
	0.50	1.00±0.12	1.01±0.11	98
Mineral water	0.00	0.21±0.05	0.23±0.0.2	-
	0.50	0.71±0.07	0.72±0.03	100
Tap water	0.00	0.32±0.04	0.33±0.04	-
	0.50	0.81±0.06	0.83±0.06	98

4. CONCLUSION

Taking all the discussed results into account, the new nanocomposite carbon paste electrode "(Au-Pd@MWCNT/Gr)-CPE" was prepared and applied for the determination of nitrite ion. The suggested modified CPE is very easy to prepare and shows high sensitivity and wide concentration range. The high degree of nitrite selectivity by the proposed sensor makes it potentially useful for monitoring concentration levels of nitrite in real samples without significant interactions with other species present in the samples. However, the suggested modified CPE has been shown to have good operating characteristics in terms of selectivity, stability, reproducibility and detection limit.

Acknowledgments

The authors wish to thank the Hamedan Branch, Islamic Azad University for financial support. The authors also wish to thank from Dr. Ali Shirzadmehr for his guidance.

REFERENCES

[1] V. Rosca, M. Duca, M. T. de Groot, and M. T. M. Koper, Chem. Rev. 109 (2009) 2209.

[2] Z. Wang, F. Liao, T. Guo, S. Yang, and C. Zeng, J. Electroanal. Chem. 664 (2012) 135.
[3] S. M. da Silva, and L. H. Mazo, Electroanalysis 10 (1998) 1200.
[4] H. Wang, P. Chen, F. Wen, Y. Zhu, and Y. Zhang, Sens. Actuators B 220 (2015) 749.
[5] C. S. Bruning Fann, and J. B. Kaneene, Vet. Hum. Toxicol. 35 (1993) 237.
[6] W. Lijinsky, and S. S. Epstein, Nature 225 (1970) 21.
[7] M. Bru, M. I. Burguete, F. Galindo, S. V. Luis, M. J. Marín, and L. Vigara, Tetrahedron Lett. 47 (2006) 1787.
[8] M. Miró, W. Frenzel, V. C. Cerdà, and J. M. Estela, Anal. Chim. Acta 437 (2001) 55.
[9] H. Liu, G. Yang, E. S. Abdel-Halim, and J. J. Zhu, Talanta 104 (2013) 135.
[10] O. Zhang, Y. Wen, J. Xu, L. Lu, X. Duan, and H. Yu, Syn. Metal. 164 (2013) 47.
[11] O. Nadzhafova, M. Etienne, and A. Walcarius, Electrochem. Commun. 9 (2007) 1189.
[12] M. I. H. Helaleh, and T. Korenaga, J. Chromatogr. B 744 (2000) 433.
[13] M. D. Croitoru, J. Chromatogr. B 911 (2012) 154.
[14] J. M. Zen, A. S. Kumar, and H. F. Wang, Analyst 125 (2000) 2169.
[15] H. Bagheri, A. Shirzadmehr, and M. Rezaei, Ionics (2016) DOI 10.1007/s11581-016-1646-9.
[16] S. S. M. Hassan, S. A. M. Marzouk, and H. E. M. Sayour, Talanta 59 (2003) 1237.
[17] S. Palanisamy, B. Thirumalraj, and S. M. Chen, J. Electroanal. Chem. 760 (2016) 97.
[18] Y. Liu, Y. Li, and X. He, Anal. Chim. Acta 819 (2014) 26.
[19] A. Afkhami, T. Madrakian, S. J. Sabounchei, M. Rezaei, S. Samiee, and M. Pourshahbaz, Sens. Actuators B161 (2012) 542.
[20] H. Bagheri, A. Afkhami, H. Khoshsafar, M. Rezaei, S. J. Sabounchei, and M. Sarlakifar, Anal. Chim. Acta 870 (2015) 56.
[21] H. Bagheri, A. Afkhami, H. Khoshsafar, M. Rezaei, and A. Shirzadmehr, Sens. Actuators B 186 (2013) 451.
[22] H. Bagheri, A. Shirzadmehr, and M. Rezaei, J. Mol. Liquid. 212 (2015) 96.
[23] A. Afkhami, H. Bagheri, H. Khoshsafar, M. Saber-Tehrani, M. Tabatabaee, and A. Shirzadmehr, Anal. Chim. Acta 746 (2012) 98.
[24] M. Mazloum-Ardakani, and A. Khoshroo, Electrochim. Acta 103 (2013) 77.
[25] L. Jiang, R. Wang, X. Li, L. Jiang, and G. Lu, Electrochem. Commun. 7 (2005) 597.
[26] M. Mazloum-Ardakani, A. Naser-Sadrabadi, and A. Khoshroo, Nano. Chem. Res. 1 (2016) 70.
[27] S. A. Shojaosadati, F. Ganji, B. Zahedi, H. A. Rafiee-pour, and H. Ghourchian, Int. J. Nanosci. Nanotechnol. 6 (2010) 195.
[28] D. Yu, L. Wei, W. Jiang, H. Wang, B. Sun, Q. Zhang, K. Goh, R. Si, and Y. Chen, Nanoscale 5 (2013) 3457.
[29] D. Zhang, Y. Fang, Z. Miao, M. Ma, X. Du, S. Takahashi, J. I. Anzai, and Q. Chen, Electrochim. Acta 107 (2013) 656.

[30] M. Behpour, S. Masoum, and M. Meshki, JNS 3 (2013) 243.
[31] J. Li, H. Xie, and L. Chen, Sens. Actuators B 153 (2011) 239.
[32] D. Ning, H. Zhang, and J. Zheng, J. Electroanal. Chem. 717–718 (2014) 29.
[33] C. Xia, X. Yanjun, and W. Ning, Electrochim. Acta 59 (2012) 81.
[34] S. Nikmanesh, M. M. Doroodmand, and M. H.Sheikhi, Int. J. Nanosci. Nanotechnol. 11 (2015) 209.
[35] M. Mazloum-Ardakani, H. Kholghi, M. A. Sheikh-Mohseni, A. Benvidi, and H. Naeimi, JNS 2 (2012) 145.
[36] S. Iijima, Nature 354 (1991) 56.
[37] R. Ramasubramaniam, J. Chen, and H. Liu, Appl. Phys. Lett. 83 (2003) 2928.
[38] A. Afkhami, A. Shirzadmehr, T. Madrakian, and H. Bagheri, Talanta 131 (2015) 548.
[39] A. Shirzadmehr, A. Afkhami, and T. Madrakian, J. Mol. Liquid. 204 (2015) 227.
[40] F. S. Ghoreishi, V. Ahmadi, and M. Samadpour, JNS 3 (2013) 453.
[41] S. Stankovich, D. A. Dikin, G. H. B. Dommett, K. M. Kohlhaas, E. J. Zimney, E. A. Stach, R. D. Piner, S. T. Nguyen, and R. S. Ruoff, Nature 442 (2006) 282.
[42] Q. Sheng, M. Wang, and J. Zheng, Sens. Actuators B 160 (2011) 1070.
[43] A. Nirmala Grace, and K. Pandian, Electrochem. Commun. 8 (2006) 1340.
[44] C. Hui-Fang, Y. Jian-Shan, L. Xiao, Z. Wei-De, and S. Fwu-Shan, Nanotechnology 17 (2006) 2334.
[45] L. Qian, and X. Yang, J. Phys. Chem. B 110 (2006) 16672.
[46] M. Ghorbanpour, JNS 3 (2013) 309.
[47] F. Doustan, A. A. Hosseini, and M. Akbarzadeh Pasha, JNS 3 (2013) 333.
[48] A. Afkhami, F. Soltani-Felehgari, T. Madrakian, and H. Ghaedi, Biosens. Bioelectron. 51 (2014) 379.
[49] F. Shahi, M. Akbarzadeh Pasha, A. A. Hosseini, and Z. S. Arabshahi, JNS 5 (2015) 87.
[50] S. Remita, M. Mostafavi, and M. O. Delcourt, Radiation Phys. Chem. 47 (1996) 275.
[51] R. Su, R. Tiruvalam, Q. He, N. Dimitratos, L. Kesavan, C. Hammond, J. A. Lopez-Sanchez, R. Bechstein, C. J. Kiely, G. J. Hutchings, and F. Besenbacher, ACS Nano 6 (2012) 6284.
[52] F. Ksar, L. Ramos, B. Keita, L. Nadjo, P. Beaunier, and H. Remita, Chem. Mater. 21 (2009) 3677.
[53] Y. Ding, F. Fan, Z. Tian, and Z. L. Wang, J. Am. Chem. Soc.132 (2010) 12480.
[54] X. Chen, H. Pan, H. Liu, and M. Du, Electrochim. Acta 56 (2010) 636.
[55] J. Yang, S. Deng, J. Lei, H. Ju, and S. Gunasekaran, Biosens. Bioelectron. 29 (2011) 159.
[56] P. Qian, S. Ai, H. Yin, and J. Li, Microchim. Acta 168 (2010) 347.
[57] C. Zhou, S. Li, W. Zhu, H. Pang, and H. Ma, Electrochim. Acta 113 (2013) 454.

[58] F. Beck, Cyclic voltammetry—simulation and analysis of reaction mechanisms. By David K. Gosser, Jr., VCH, New York (1993).
[59] F. Pourfayaz, S. Iranpour, and O. Shojaei, Int. J. Nanosci. Nanotechnol. 11 (2015) 219.
[60] Y. W. Lee, M. Kim, Y. Kim, S. W. Kang, J. H. Lee, and S. W. Han, J. Phys. Chem. C 114 (2010) 7689.
[61] A. A. Ensafi, T. Khayamian, and S. S. Khaloo, Int. J. Food Sci. Technol. 43 (2008) 416.
[62] M. Shariati-Rad, M. Irandoust, and S. Mohammadi, Spectrochim. Acta Part A 149 (2015) 190.
[63] J. M. Zen, A. S. Kumar, and H. W. Chen, Electroanalysis 13 (2001) 1171.
[64] A. A. Rafati, A. Afraz, A. Hajian, and P. Assari, Microchim. Acta 181 (2014) 1999.
[65] M. R. Ganjali, N. Motakef-Kazami, F. Faridbod, S. Khoee, and P. Norouzi, J. Hazard. Mater. 173 (2010) 415.